Regulation of blood–testis barrier dynamics by TGF-β3 is a Cdc42-dependent protein trafficking event

Elissa W. P. Wong[a], Dolores D. Mruk[a], Will M. Lee[b], and C. Yan Cheng[a,1]

[a]Center for Biomedical Research, Population Council, New York, NY 10065; and [b]School of Biological Sciences, University of Hong Kong, Hong Kong SAR, China

Edited by Ryuzo Yanagimachi, The Institute for Biogenesis Research, University of Hawaii, Honolulu, HI, and approved May 10, 2010 (received for review January 26, 2010)

In the testis, the blood–testis barrier (BTB) is constituted by specialized junctions between adjacent Sertoli cells in the seminiferous epithelium near the basement membrane. Although the BTB is one of the tightest blood–tissue barriers in the mammalian body, it undergoes extensive restructuring at stage VIII of the seminiferous epithelial cycle to facilitate the transit of preleptotene spermatocytes. Thus, meiosis and postmeiotic germ cell development take place in the seminiferous epithelium behind the BTB. Cytokines (e.g., TGF-β3) are known to regulate BTB dynamics by enhancing the endocytosis of integral membrane proteins and their intracellular degradation. This thus reduces the levels of proteins above the spermatocytes in transit at the BTB, causing its disruption after testosterone-induced new tight junction (TJ) fibrils are formed behind these cells. By using Sertoli cells cultured in vitro with an established TJ permeability barrier that mimicked the BTB in vivo, Cdc42 was shown to be a crucial regulator that mediated the TGF-β3–induced BTB disruption. TGF-β3 was shown to activate Cdc42 to its active GTP-bound form. However, an inactivation of Cdc42 by overexpressing its dominant-negative mutant T17N in Sertoli cell epithelium was shown to block the TGF-β3–induced acceleration in protein endocytosis. Consequently, this prevented the disruption of Sertoli cell TJ permeability barrier and redistribution of TJ proteins (e.g., CAR and ZO-1) from the cell–cell interface to cell cytosol caused by TGF-β3 on Sertoli cell BTB integrity. In summary, Cdc42 is a crucial regulatory component in the TGF-β3–mediated cascade of events that leads to the disruption of the TJ fibrils above the preleptotene spermatocytes to facilitate their transit.

cytokines | GTPases | protein endocytosis | seminiferous epithelial cycle | spermatogenesis

In mammalian testis, the seminiferous epithelium is segregated into the basal and apical compartments by the blood–testis barrier (BTB), which is created by coexisting tight junction (TJ), basal ectoplasmic specialization [ES, a testis-specific atypical adherens junction (AJ) type], and desmosome gap junctions between adjacent Sertoli cells near the basement membrane (1, 2). At stage VIII of the seminiferous epithelial cycle, the BTB undergoes extensive restructuring to allow the transit of preleptotene spermatocytes from the basal to the apical compartment. At the same time, preleptotene spermatocytes differentiate into leptotene and zygotene spermatocytes (3) so that meiosis and postmeiotic germ cell development can take place in the apical compartment behind the BTB (2). While the BTB undergoes this cyclic restructuring throughout spermatogenesis, the immunological barrier conferred by the BTB is maintained at all time to segregate the postmeiotic germ cell development from the host immune system to avoid the production of antibodies against germ cell–specific antigens that attack its own sperms. Previous studies have shown that cytokines (e.g., TGF-β2 and TGF-β3) and testosterone are working in concert to facilitate the transit of spermatocytes at the BTB while maintaining the immunological barrier (2, 4). For instance, testosterone maintains the immunological barrier by inducing de novo synthesis of junction proteins (e.g., claudins and occludin) (5–7) as well as transcytosis of proteins from other sites of the cells to promote the assembly of "new" TJ fibrils behind a spermatocyte in transit (4). Conversely, cytokines enhance endocytosis of integral membrane proteins above a spermatocyte in transit and target the internalized TJ fibril proteins for intracellular degradation (4, 8), thereby destabilizing the "old" BTB ultrastructure to facilitate their transit (2). However, the regulatory component(s) that modulates these events, such as the TGF-β–induced enhancement in protein endocytosis, remains virtually unknown. Previous studies have implicated the Rho family small GTPase Cdc42 in regulating protein trafficking events, such as endocytosis and exocytosis, besides its roles as an actin cytoskeleton regulator (1). Although studies have shown that an alteration of Cdc42 activity, such as by overexpression of dominant-negative or constitutive-active mutant of Cdc42, induces changes in protein trafficking in cells, the upstream regulators that control Cdc42 activity in this process are unknown (1). Here, we sought to examine whether TGF-β3, when used at a concentration similar to the level at the BTB microenvironment in vivo (8), is an upstream physiological stimulus that activates Cdc42, and if the activation state of Cdc42 is essential for mediating TGF-β3–induced acceleration of protein endocytosis at the BTB. We also examined if Cdc42 determines the extent of endocytosed integral membrane proteins that should be recycled and targeted to the cell surface. In short, we sought to investigate if the TGF-β3–induced Sertoli cell BTB disruption is mediated by Cdc42 via its effects on protein trafficking.

Results

Localization of Cdc42 at the BTB Is Stage-Specific with Considerably Diminished Expression at Stage VII to VIII of the Epithelial Cycle, Coinciding with BTB Restructuring. To understand whether Cdc42 is involved in regulating BTB dynamics, its localization in rat testis was first characterized by immunohistochemistry. Frozen testis cross-sections from adult rats were stained with an anti-Cdc42 antibody (Fig. 1A, *i–vii*). This antibody specifically detected Cdc42 by immunoblotting using lysates obtained from rat testes and Sertoli cells (Fig. 1*A*, *vii*). Cdc42 was ubiquitously expressed in the entire seminiferous epithelium (Fig. 1*A*, *i*). This finding is consistent with earlier studies that show that Cdc42 regulates various cellular processes, such as actin dynamics and cell polarity (1). At higher magnifications, Cdc42 was found to be prominently expressed near the basement membrane, consistent with the localization of the BTB (Fig. 1*A*, *ii*, black arrowheads). Furthermore, a stage-specific expression pattern was observed (Fig. 1*A*, *i–v*). Notably, the staining of Cdc42 at the BTB in stage V tubule was weaker compared with tubules at stage X-XIII

Author contributions: E.W.P.W. and C.Y.C. designed research; E.W.P.W. and C.Y.C. performed research; E.W.P.W., D.D.M., W.M.L., and C.Y.C. contributed new reagents/analytic tools; E.W.P.W., D.D.M., and C.Y.C. analyzed data; and E.W.P.W. and C.Y.C. wrote the paper.

The authors declare no conflict of interest.

This article is a PNAS Direct Submission.

To whom correspondence should be addressed. E-mail: y-cheng@popcbr.rockefeller.edu.

This article contains supporting information online at www.pnas.org/lookup/suppl/doi:10.1073/pnas.1001077107/-/DCSupplemental.

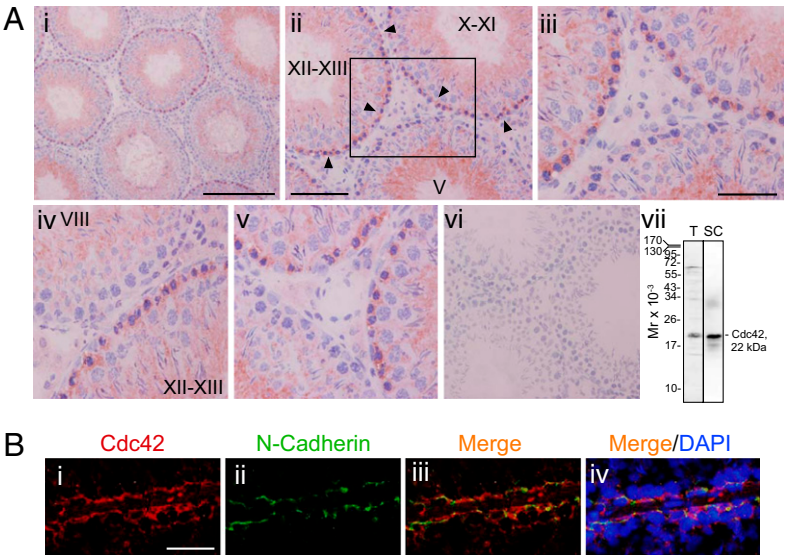

Fig. 1. Stage-specific expression of Cdc42 at the BTB in adult rat testis. (*A*, *i–v*) Immunohistochemistry was performed using frozen testis sections. The specificity of this antibody in testis (T) and Sertoli cell (SC) were illustrated in *vii*. (*i*) Cdc42 was localized in the seminiferous epithelium with stage-specific expression at the BTB but it was absent in stage VIII tubules. (*ii*) Magnified micrograph showing Cdc42 was detected in the Sertoli cell cytoplasm that extended toward the edge of the tubule lumen but was predominantly localized at the BTB (black arrowheads). (*iii*) Magnified view of the boxed area in *b* showing Cdc42 was highly expressed at the BTB with its expression began to diminish at stage V. (*iv* and *v*) Reduced level of Cdc42 at the BTB persisted from stage VI to VIII. At stage VIII, Cdc42 at the BTB was virtually undetectable. (*vi*) Control section in which normal chicken IgY was replaced with the anti-Cdc42 antibody. [Scale bars: *i*, 100 μm; *ii* (applies to *vi*), 40 μm; *iii* (applies to *iv* and *v*), 20 μm.] (*B*) Colocalization of Cdc42 (red, *i*) with basal ES protein N-cadherin (green, *ii*) at the BTB (*iii*). Nuclei were stained with DAPI (blue, *iv*). [Scale bars: 10 μm in *i* (applies to *ii–iv*).]

(Fig. 1*A*, *c*, is a magnified view of the boxed area shown in Fig. 1*A*, *ii*). However, this diminished staining was most obvious and drastic at stage VII-VIII (Fig. 1*A*, *i* and *iv*) when the BTB undergoes extensive restructuring to facilitate the transit of preleptotene spermatocytes. When the anti-Cdc42 antibody was replaced with normal chicken IgY, no positive signal was observed (Fig. 1*A*, *vi*) illustrating the specificity of the staining results in Fig. 1*A*, *i–v*. To further validate the localization of Cdc42 at the BTB, dual-labeled immunofluorescence analysis was performed to colocalize Cdc42 with a known BTB marker. Consistently, Cdc42 (Fig. 1*B*, *i*, red) was shown to colocalize with the basal ES marker N-cadherin (Fig. 1*B*, *ii*, green) at the BTB (Fig. 1*B*, *iii* and *iv*).

Cdc42 Is Activated in Sertoli Cell Epithelium upon TGF-β3 Stimulation. TGF-β3 is a known regulator of BTB (2), to test the possibility that Cdc42 is a downstream mediator of TGF-β3, we first examined if TGF-β3 affects the activation of Cdc42 in a Sertoli cell culture system known to establish functional and structural barrier that mimics the BTB in vivo (9). As Cdc42 switches between active (i.e., GTP-bound) and inactive (i.e., GDP-bound) states, we performed a pull-down assay using GST-p21–binding domain (i.e., PBD) of PAK-1 to precipitate active Cdc42 (Cdc42-GTP). Isolated Sertoli cells were cultured in F12/DMEM for 4 d to form an intact cell epithelium before being stimulated with 4 ng/mL TGF-β3, at a concentration similar to its level at the BTB microenvironment in vivo (8). It was found that TGF-β3 transiently activated Cdc42 at 5 and 20 min after Sertoli cells were exposed to TGF-β3 (Fig. 2 *A* and *B*). However, prolonged stimulation by TGF-β3 for 60 min significantly decreased the level of active Cdc42 versus its basal level at 0 min (Fig. 2 *A* and *B*). In addition, the inactivation of Cdc42 at 60 min was accompanied by a mild but significant decrease in the total Cdc42 (Fig. 2 *A* and *C*). Previous studies have shown that TGF-β3 disrupts the Sertoli cell TJ barrier (10). However, it is not known if TGF-β3 disrupts the TJ barrier within 24 h after cells are exposed to TGF-β3. Thus, 4 ng/mL TGF-β3 was added to the Sertoli cell epithelium on day 4 when functional TJ had been established (Fig. 2*D*). Interestingly, the TJ barrier was not disrupted when the transepithelial electrical resistance (TER) as quantified at 15 and 60 min after the addition of TGF-β3 (Fig. 2*D*) when Cdc42 was activated before this time at 5 to 20 min (Fig. 2*A* vs. Fig. 2*D*). Instead, the TJ barrier was visibly disrupted by 3 h and thereafter (Fig. 2*D*). These findings implicate that Cdc42 activation maybe necessary for the subsequent effects of TGF-β3 on the Sertoli cell TJ barrier function.

Cdc42 Is Required to Mediate TGF-β3–Induced Activation of p38 MAPK. The findings that Cdc42 is localized at the BTB (Fig. 1) and TGF-β3 regulates its activation state (Fig. 2) implicates that Cdc42 is a crucial mediator of TGF-β3–induced BTB disruption. To test this hypothesis, we altered the activation state of Cdc42 by expressing full-length Cdc42 or dominant-negative Cdc42 mutant T17N in primary Sertoli cells and investigate if there is

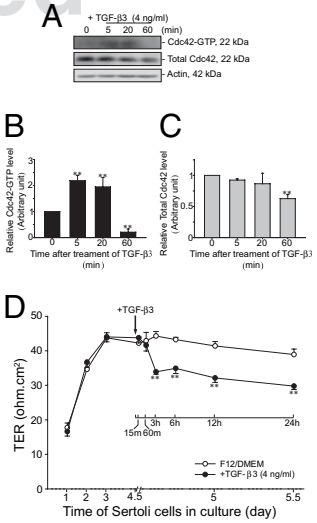

Fig. 2. TGF-β3 activates Cdc42 in Sertoli cells. (*A*) Sertoli cells were cultured for 4 d, thereafter, cells were stimulated with TGF-β3 (4 ng/mL) for 5 to 60 min. GTP-bound Cdc42 (active form) was quantified. Equal amount of proteins were probed with an anti-Cdc42 antibody to estimate total Cdc42, and the same blot was stripped and probed with an anti-actin antibody to assess equal protein loading. TGF-β3 transiently stimulated Cdc42 at 5 and 20 min after treatment. At 60 min, both total and active Cdc42 were significantly decreased versus controls. Composite data from three experiments for Cdc42-GTP (*B*) and total Cdc42 (*C*) are shown. Protein level at 0 min was arbitrarily set at 1. Each bar is a mean ± SD; $^{**}P < 0.01$. (*D*) Sertoli cells were cultured at 1.2×10^6 cells/cm^2 on Matrigel-coated bicameral units and the TJ barrier function was monitored by quantifying the TER across the cell epithelium. TGF-β3 (4 ng/mL) was added to the units on day 4.5 (arrow). This experiment was repeated three times. Each data point is a mean ± SD; $^{**}P < 0.01$.

any change in steady-state levels of integral membrane proteins at the BTB in the presence or absence (control) of TGF-β3. The dominant-negative mutant of Cdc42 contained a site-specific mutation that converted amino acid residue 17 from Thr (T) to Asn (N). This thereby sequesters guanine nucleotide exchange factors to prevent endogenous Cdc42 from being activated (11). Transfection was performed 2 d after Sertoli cell isolation to allow functional TJ barrier and ultrastructures of BTB to form (12). Overexpression of Cdc42 and T17N in primary Sertoli cells was confirmed by RT-PCR (Fig. 3*A*, *i*) and immunoblotting (Fig. 3*A*, *ii*). An approximately 8-fold and 2.5-fold increase in Cdc42 mRNA and protein versus vector pCIneo control were observed, respectively. Two days after transfection, cell lysates were harvested to examine protein levels of several BTB-associated proteins by immunoblotting. It was found that levels of several TJ (e.g., occludin, JAM-A, CAR, and ZO-1) and basal ES proteins (e.g., N-cadherin, α-catenin, β-catenin, and γ-catenin) remained unaltered after overexpression of Cdc42 and T17N versus pCIneo vector control (Fig. 3 *B–D*). Furthermore, when transfected cells were treated with TGF-β3 (4 ng/mL) for 1 h, no significant changes in protein levels were noted (Fig. 3 *B–D*). Collectively, these findings suggest that overexpression of Cdc42 or its dominant-negative mutant T17N in Sertoli cells did not affect the steady-state levels of integral membrane proteins at the BTB. It is noted that TGF-β3 perturbs the Sertoli cell BTB function via p38 MAPK (10, 13). Therefore, we examined the phosphorylation level of p38 MAPK after overexpression of Cdc42 or T17N in the presence or absence of TGF-β3 (Fig. 3 *E* and *F*). Consistent with the previous findings, TGF-β3 enhanced phosphorylation of p38 MAPK after TGF-β3 stimulation in vector control cells. Unexpectedly, overexpression of Cdc42 alone also activated p38 MAPK, possibly as a result of the increased level of Cdc42 to transduce signal in the p38 MAPK pathway. However, the level of phosphorylated-p38 MAPK was not affected by T17N overexpression. Significantly, inhibition of endogenous Cdc42 by T17N blocked TGF-β3–induced p38 MAPK phosphorylation (Fig. 3 *E* and *F*).

Active Cdc42 Is Essential for the TGF-β3–Enhanced Protein Endocytosis at the BTB. TGF-β3 is known to disrupt Sertoli cell BTB function by enhancing endocytosis of integral membrane proteins at the BTB (8). To address whether TGF-β3 induces protein internalization via activation of Cdc42, we performed an endocytosis assay using Cdc42- or T17N-expressing Sertoli cells in the presence or absence of TGF-β3 using Sertoli cells cultured for 4 d with an intact epithelium. Cell surface proteins of Sertoli cells expressing vector control (pCIneo), Cdc42, or T17N were biotinylated with approximately equal amounts of biotinylated proteins (e.g., occludin and CAR) were found on the cell surface in these cells (Fig. S1). Sertoli cells were then incubated with or without TGF-β3 (4 ng/mL) for 5, 20, and 60 min. Internalized proteins were evaluated by recovering cell surface biotinylated proteins on streptavidin beads. We quantified the rate of protein internalization by calculating the percentage of endocytosed protein, which is defined as the level of internalized proteins over

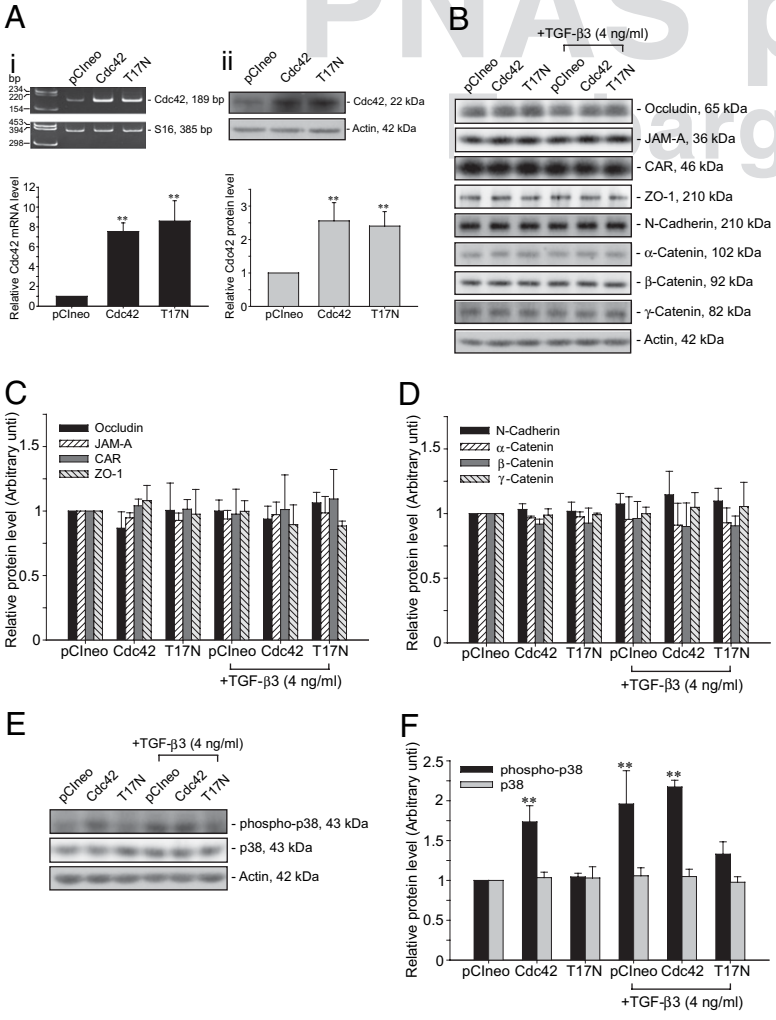

Fig. 3. Activation of p38 MAPK by TGF-β3 is mediated by Cdc42. (*A*) Sertoli cells were cultured at 0.5×10^6 cells/cm^2 for 2 d to establish a functional TJ barrier before transfected with vector control (pCIneo), full-length Cdc42 (Cdc42), or dominant-negative mutant of Cdc42 (T17N). (*i*) Total RNA was extracted 12 h posttransfection and treated with DNase I to remove any possible genomic DNA contamination, and the expression level of Cdc42 mRNA was monitored by RT-PCR with S16 served as a loading control (*Upper*). (*ii*) Immunoblotting was performed 2 d after transfection to assess the increase in Cdc42 and T17N protein levels. Lower panels in *a* and *b* are composite results from three experiments. (*B*) Protein lysates were harvested 2 d after transfection. Before termination, cells were treated with or without TGF-β3 (4 ng/mL) for 60 min. Steady-state levels of BTB-associated proteins were then assessed by immunoblotting. (*E*) Phosphorylation of p38 MAPK was quantified by immunoblotting using an anti–phospho-p38 antibody. Addition of TGF-β3 in vector control (pCIneo) cells or overexpression of Cdc42 alone resulted in phosphorylation of p38 MAPK. Activation of p38 MAPK was Cdc42-dependent as overexpression of the dominant-negative mutant of T17N prevented its activation induced by TGF-β3. Total p38 MAPK level remained unchanged in all groups. (*C*, *D*, and *F*) Bar graphs (mean ± SD) show composite results of three experiments. Cdc42 mRNA (*A*, *Lower*) and protein (*C*, *D*, and *F*) levels were normalized against S16 and actin, respectively, with the mRNA and protein level from cells transfected with pCIneo (vector alone) arbitrarily set at 1; $^{**}P < 0.01$.

total cell surface proteins that were biotinylated without stripping. As shown in Fig. 4 *A*, *B*, and *E*, Sertoli cells expressing full-length Cdc42 displayed an increase in endocytosis of occludin and CAR versus vector control. In contrast, expression of T17N in Sertoli cells did not change the rate of endocytosis significantly versus control cells (Fig. 4 *A*, *B*, and *E*). Similar to the previously published results (8), TGF-β3 promoted endocytosis of occludin and CAR (Fig. 4 *A*, *C*, and *F*). Besides, we found that by overexpressing Cdc42 and stimulating the cells with TGF-β3, it has an additive effect on enhancing protein endocytosis (Fig. 4 *A*, *D*, and *G*). Importantly, Sertoli cells lacking active Cdc42, by expressing dominant-negative mutant T17N, was shown to eliminate the stimulatory effect of TGF-β3 on protein endocytosis (Fig. 4 *A*, *D*, and *G*). Collectively, these data demonstrated that the disruptive effects of TGF-β3 on BTB dynamics via an increase in protein endocytosis at the BTB is mediated by Cdc42. Furthermore, these findings also illustrated that, although protein endocytosis at the Sertoli cell BTB per se under basal condition is not entirely dependent on Cdc42, the TGF-β3–induced protein endocytosis is dependent on Cdc42.

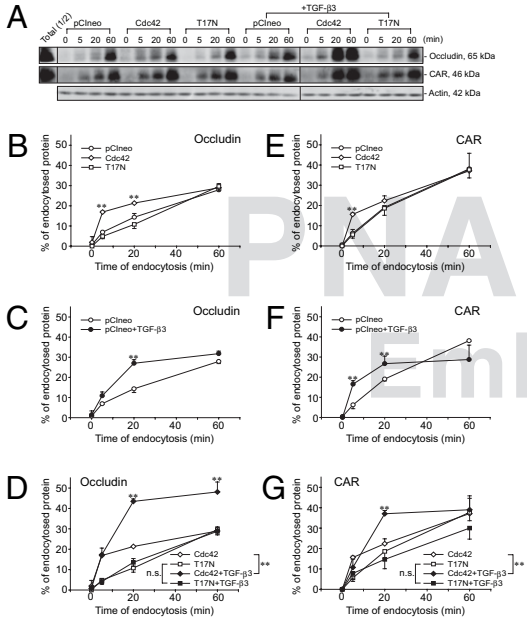

Fig. 4. TGF-β3–mediated acceleration of protein endocytosis at the BTB requires active Cdc42. (*A*) Sertoli cells expressing vector control (pCIneo), Cdc42, or dominant-negative Cdc42 (T17N) were used for endocytosis assay 2 d after transfection. Cells were biotinylated at 4 °C and incubated in the presence *or* absence of TGF-β3 (4 ng/mL) for 0, 5, 20, or 60 min at 35 °C to allow protein endocytosis. At specified time points, biotin on cell surface proteins that were not internalized were stripped. Cell lysates were harvested in RIPA lysis buffer. Biotinylated proteins that were endocytosed were recovered by using NeutrAvidin beads for immunoblotting. Half of the total cell surface biotinylated proteins, without stripping with MESNA buffer, were used to estimate the percentage of endocytosed protein. The blots for occludin and CAR shown herein are representative of three experiments. Actin served as a loading control. *B–D* and *E–G* are the corresponding data for occludin and CAR. (*B* and *E*) Results expressed as the percentage of endocytosed protein normalized against total cell surface biotinylated protein. Transient overexpression of Cdc42 enhanced protein endocytosis whereas overexpression of T17N did not affect kinetics of protein internalization versus vector control, illustrating that Cdc42 facilitated but was not essential for protein endocytosis at the BTB under normal physiological conditions. (*C* and *F*) Addition of TGF-β3 increased the rate of protein endocytosis versus vector control. Each time point is mean ± SD; $^{**}P < 0.01$ (pCIneo vs. Cdc42, T17N or pCIneo+TGF-β3). (*D* and *G*) Treatment of Sertoli cells overexpressing Cdc42 with TGF-β3 further enhanced endocytosis. However, overexpression of T17N abolished TGF-β3–induced enhancement of protein endocytosis. Each time point is a mean ± SD; $^{**}P < 0.01$ (Cdc42 vs. Cdc42+TGF-β3); n.s., no significant change (T17N vs. T17N+TGF-β3).

Protein Recycling to the Cell Surface Is Impaired by an Inactivation of Cdc42. The amount of proteins that remains at the intercellular junctions is the net result of protein endocytosis, recycling, transcytosis, and intracellular degradation. Thus, we next investigated if Cdc42 affects recycling of endocytosed proteins to cell surface. Cell surface proteins were biotinylated and cells were incubated at 18 °C for 2 h to allow accumulation of endocytosed proteins in early or sorting endosomes (14). Biotin that remained on cell surface proteins that were not endocytosed was removed by 2-mercaptoethane sulfonate (MESNA) stripping buffer. Biotinylated proteins that were internalized into cell cytosol were allowed to recycle back to the plasma membrane for 1 h, which was subsequently extracted to track the amount of recycled biotinylated proteins on the cell surface. Fig. S2 illustrates that an equal amount of protein was used the recycling assay shown in Fig. 5. In line with the previously published results, TGF-β3 impaired targeting of endocytosed proteins back to the cell surface. Instead, they underwent endosome-mediated protein degradation (4) (Fig. 5*A*), which eventually led to a disruption of Sertoli cell TJ barrier (Fig. 5*A* and Fig. 2*D*). However, in this study, it was shown that overexpression of T17N alone also inhibited protein recycling but to a lesser extent versus control cells treated with TGF-β3 (T17N vs. pCIneo+TGF-β3; Fig. 5*A*). Interestingly, it is noted that there was no significant change in recycling of CAR when T17N-expressing cells were treated with TGF-β3.

Inactivation of Cdc42 Blocks TGF-β3–Induced Disruption of Cell Junctions at the BTB. We next characterized if an inactivation of Cdc42 would lead to any phenotypic changes in the Sertoli cell TJ barrier and protein distribution at the cell–cell interface (Fig. S3). Overexpression of dominant-negative T17N was performed on day 2 by transfecting Sertoli cells with an established TJ barrier. On day 4.5, 4 ng/mL TGF-β3 was added in both the apical and basal compartments of the bicameral units for 24 h (Fig. 6*A*). In vector control cells, TGF-β3 significantly perturbed the TJ barrier by 3 h which persisted until the end of the experiment. Conversely, T17N expression prevented TGF-β3–induced TJ barrier disruption (Fig. 6*A*). We next determined if these changes in TJ barrier disruption would be reflected by an alteration in the localization of junction proteins at the cell–cell interface. Transfected cells were denoted by vectors that were fluorescently labeled by Cy3 (Fig. 6*B* and *C*, red). CAR (Fig. 6*B*, green) and ZO-1 (Fig. 6*C*, green) was localized at the cell–cell interface in control cells without treatment of TGF-β3 that formed an almost undisrupted barrier. However, cells that were treated with TGF-β3 (4 ng/mL) displayed a dis-

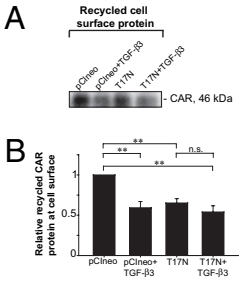

Fig. 5. Inactivation of Cdc42 in Sertoli cell epithelium perturbs protein recycling. (*A*) Recycling of proteins from cytosol to plasma membrane was assessed as described in *Materials and Methods*. Overexpression of T17N resulted in a decrease in recycling of proteins, such as CAR, back to cell surface. Also, treatment of Sertoli cell BTB with TGF-β3 perturbed CAR protein recycling. However, inactivation of Cdc42 neither blocked nor potentiated TGF-β3–induced disruption of protein recycling. (*B*) Composite data of *A* is shown.

ruption of CAR and ZO-1 staining at the Sertoli cell junctions (Fig. 6*B* and *C*). In cells with Cdc42 overexpression, a mild disruption of CAR localization (Fig. 6*B*) at the cell junction was noted, and more ZO-1 also redistributed near the cell surface (yellow arrowheads in Fig. 6*B*) to cytosol (white arrowheads in Fig. 6*B*). These findings are consistent with the results indicating that both TGF-β3 treatment and Cdc42 overexpression resulted in enhanced endocytosis as shown in Fig. 4 *A*–*G*. However, both CAR and ZO-1 remained at the cell–cell interface in Sertoli cells overexpressing T17N (Fig. 6 *B* and *C* and Fig. S3). In agreement with the additive effect in endocytosis by treating Cdc42-expressing cells with TGF-β3, a more severe disruption in CAR and ZO-1 localization was noted (Fig. 6 *B* and *C*, green). Based on results shown in Fig. 4 *A* and *D*–*G*, TGF-β3–induced enhancement in endocytosis was abolished when Cdc42 was inactivated. This finding was confirmed by data shown in Fig. 6 *A* and *B* in which overexpression of T17N in the epithelium would render these cells nonresponsive to the disruptive effects of TGF-β3. For instance, the disruptive effect of TGF-β3 in redistributing CAR and ZO-1 from the cell surface to cytosol was blocked when Cdc42 was inactivated (Fig. 6 *B* and *C*).

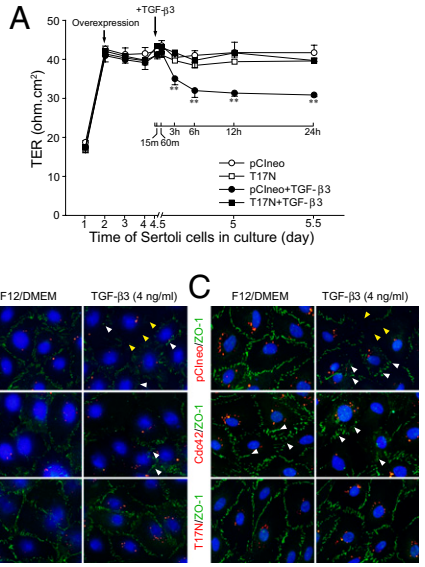

Fig. 6. Sertoli cell junction disruption induced by TGF-β3 is blocked by inactivation of Cdc42. (*A*) Sertoli cells were cultured at 1.2×10^6 cells/cm^2 on bicameral units and transfected with vector control pCIneo or T17N on day 2 after plating; 2.5 d thereafter (i.e., on day 4.5), cells were treated with or without TGF-β3 (4 ng/mL) and the TJ barrier function was monitored by TER measurement. Expression of T17N alone did not result in change in TER versus vector control (pCIneo). Addition of TGF-β3 in vector control cells resulted in a significant decrease in TER, illustrating TJ barrier disruption. Conversely, overexpression of T17N blocked the disruptive effect of TGF-β3 on the TJ barrier. (*B* and *C*) Sertoli cells transfected with vector control (pCIneo), Cdc42, or T17N were treated with or without 4 ng/mL of TGF-β3 for 60 min. Transfected cells were tracked by fluorescently labeling plasmids with Cy3 (red). Cells were fixed and stained with either an anti-CAR antibody (green) (*B*) or an anti–ZO-1 antibody (green) (*C*). Nuclei were visualized by DAPI (blue). Overexpression of Cdc42 caused a mild redistribution of CAR (*B*) and ZO-1 (*C*) from the Sertoli–Sertoli cell interface to cytosol versus pCIneo. Treatment of control cells with TGF-β3 disrupted the localization of CAR (*B*) and ZO-1 (*C*) at the cell–cell interface in both control and Cdc42-overexpressed cells, causing them to relocate from the cell surface (yellow arrowhead) to cytosol (white arrowhead). Whereas overexpression of Cdc42 worsened junction damage induced by TGF-β3, inactivation of Cdc42 by overexpressing T17N blocked the TGF-β3–induced junction disruption, confirming results in *A*.

Discussion

TGF-β3–Accelerated Protein Endocytosis That Leads to BTB Disruption Is Mediated by Cdc42. Cdc42 was shown to be a downstream effector necessary for the TGF-β3–induced BTB restructuring. TGF-β3 appears to exert its effects by first activating Cdc42 to its GTP-bound form, which in turn enhances protein endocytosis at the BTB to disrupt the TJ barrier. Although overexpression of Cdc42 in Sertoli cells facilitates protein endocytosis, its inactivation in Sertoli cells, such as by overexpressing T17N, did not affect the kinetics of protein endocytosis at the BTB or the distribution of CAR and ZO-1 at the cell surface as reported herein. This illustrates that the function of Cdc42 on endocytosis under normal physiological conditions can be superseded by other GTPases, as several GTPases are involved in endocytic vesicle-mediated protein trafficking (15, 16). However, Cdc42 is absolutely needed for TGF-β3–mediated Sertoli cell BTB disruption and this effect cannot be superseded by other GTPases, as supported by several observations. First, Cdc42 was activated by TGF-β3 preceding the TJ barrier disruption. Second, inactivation of Cdc42 via an overexpression of T17N in Sertoli cells would render a loss of response of the cell epithelium to TGF-β3–induced acceleration in protein endocytosis. Third, perhaps most importantly, an inactivation of Cdc42 would lead to a loss of response of the Sertoli cells to the disruptive effects of TGF-β3 regarding the TJ barrier function. These findings are further supported by immunofluorescence analysis, which showed that TGF-β3 was effective to induce relocation of CAR and ZO-1 from the cell–cell interface to cytosol, but it failed to induce similar redistribution of CAR in Sertoli cells when Cdc42 was inactivated. Collectively, these data demonstrate unequivocally the pivotal role of Cdc42 in mediating the regulatory function of TGF-β3 in BTB dynamics. However, it is of interest to note that the expression of Cdc42 in the seminiferous epithelium as demonstrated by immunohistochemistry using an antibody against total Cdc42 is stage-stage, where its expression at the BTB is lowest at stage VIII whereas TGF-β3 expression at this site is highest at this stage (13). If Cdc42 is so crucial to TGF-β3 action at stage VIII, why would its expression level be reduced at the BTB at this stage? We offer the following explanation. The antibody used in our study stained total Cdc42, yet most of the Cdc42 at the BTB at this stage would have been activated by TGF-β3, as shown in Fig. 2*A*, when its expression was highest at the BTB site at stage VIII as reported earlier (13). As activated Cdc42 would have a different antigenic configuration, this makes it possibly unrecognizable by the anti–total Cdc42 antibody. These findings are analogous to an earlier report illustrating total FAK is localized mostly at the BTB, but its active phosphorylated forms (e.g., p-FAK-Tyr^{397} and p-FAK-Tyr^{576}) are restricted to the apical ES (17), where the anti–total FAK failed to detect these two activated forms at this site. Additionally, germ cells may regulate the expression and/or the activation of Sertoli cell Cdc42 in the seminiferous epithelium microenvironment, such as the BTB.

Cdc42 Is Not Involved in TGF-β3–Mediated Protein Recycling Events. In the present study, Cdc42 was shown to be involved in protein recycling, analogous to earlier studies in MDCK cells reporting that a deletion (18) or inactivation of Cdc42 (19) would impede protein recycling back to the cell surface. However, Cdc42 is not essential in basal and TGF-β3–mediated protein recycling. For instance, cell–cell junctions remain intact in T17N-expressing cells despite a decrease in recycling of CAR back to the cell surface. Furthermore, when control cells were treated with TGF-β3, a disruption of CAR and ZO-1 localization was observed when there is an increase in endocytosis and a decrease in protein recycling. This conclusion is further strengthened from the immunofluorescence staining and TER measurement data, which show that overexpression of T17N is able to reverse the disruptive effects of TGF-β3 on the TJ barrier by blocking the increase in TGF-β3–mediated endocytosis. These results collec-

tively reveal that the role of Cdc42 on mediating TGF-β3–induced protein endocytosis is more profound and is able to supersede its effect on recycling of proteins to cell surface. Conversely, if protein recycling at the BTB is dependent entirely on Cdc42, the TJ barrier function would have been disrupted after overexpression of T17N in Sertoli cells because of the impairment in protein recycling. These findings are consistent with earlier studies that show an inactivation of Cdc42 did not result in morphological changes in TJ fibrils in MDCK cells (19, 20). It is likely that, although Cdc42 activity is needed for protein recycling at the BTB, other small GTPases, such as Rab proteins (e.g., Rab13) (21, 22) play a more dominant role on protein recycling, and TGF-β3 can also mediate its effects on recycling via one of these other GTPases.

Cdc42 Are Working with Polarity Proteins to Regulate BTB Dynamics. During the infiltration of *Neisseria meningitidis* across the blood–brain barrier that causes meningitis, an activation of Cdc42 was detected that induced protein endocytosis in the microvessel endothelium to increase TJ permeability to facilitate the bacterial entry (23). To prevent hemorrhage, the bacterial pili also activated Cdc42 behind their entry site to recruit polarity complex Par3/Par6/aPKC to reestablish the endothelial barrier by relocating the endocytosed TJ and AJ proteins via transcytosis to the site (23). In fact, Cdc42 is known to be involved in targeting of proteins to the basolateral domain of epithelial cells (19, 24). Together with the previously published results in which Par6 and 14–3-3 (also known as Par5) were shown to be involved in endocytic vesicle-mediated protein trafficking at the BTB (25), it is likely that Cdc42 is working in concert with Par6 and 14–3-3 to play a dual role in regulating BTB dynamics. First, Cdc42 facilitates TGF-β3–ehanced endocytosis to disrupt "old" TJ-fibrils above the migrating spermatocytes. Second, it also helps to target the endocytosed proteins to the "new" BTB site below the spermatocytes via transcytosis, likely working with Par6 and 14–3-3. This thus maintains the BTB integrity during the transit of spermatocytes.

Materials and Methods

Animals and Antibodies. The use of Sprague-Dawley rats was approved by the Rockefeller University Animal Care and Use Committee (protocols 06018 and 09016). Antibodies used in this study are listed in Table S1.

General Methods. Primary Sertoli cell cultures, DNA transfection, cell staining, preparation of cDNA constructs, Cdc42 activation assay, immunohistochemistry, fluorescence microscopy, TJ barrier function assessment, and statistical analysis are described in *SI Materials and Methods*.

Endocytosis Assay. Endocytosis assay was performed as described (4, 25). Cell lysates were harvested in RIPA buffer (50 mM Tris/HCl, 150 mM NaCl, 5 mM EGTA, 0.2% SDS, 1% Triton X-100, 1% sodium deoxycholate, and 2 mM N-ethylmaleimide, pH 8), with 1 μg/mL aprotinin, 1 μg/mL leupeptin, 2 mM PMSF, and 15 μL/mL each of phosphatase inhibitor mixtures 1 and 2 (Sigma). Biotinylated proteins were recovered by Ultralink Immobilized NeutrAvidin Plus beads (Pierce) and subjected to SDS/PAGE and immunoblotting.

Recycling Assay. Cell surface proteins were biotinylated at 4 °C as described (4). Cells were then incubated at 18 °C for 2 h to allow internalization and accumulation of biotinylated proteins in early or sorting endosomes (14). Biotinylated proteins that were not endocytosed were stripped by 50 mM 2-mercaptoethanesulfonate MESNA buffer (15). F12/DMEM with or without TGF-β3 (4 ng/mL) was added for 1 h at 35 °C and plasma membrane was extracted. In brief, cells were scraped from 100-mm plates in 250 mM sucrose, 20 mM Tris-HCl, 2 mM EGTA, pH 7.5, freshly supplemented with protease and phosphatase inhibitors (lysis buffer). Cells were sonciated and unbroken cells and nuclei were removed by centrifugation at 3,000 × *g* for 5 min. Postnuclei supernatant was centrifuged at 17,000 × *g* for 20 min, and the pellet was resuspended in 100 μL of lysis buffer and overlaid on 1 mL of 1.12 M sucrose solution. Ultracentrifugation was performed at 100,000 × *g* for 1 h and the top layer of the sucrose cushion was enriched with plasma membrane. Subsequently, the top layer was collected and centrifuged at 40,000 × *g* for 30 min, and the pellet (plasma membrane) was dissolved in RIPA buffer for affinity precipitation by NeutrAvidin Plus beads.

ACKNOWLEDGMENTS. This work was supported by National Institutes of Health/National Institute of Child Health and Human Development Grants R01 HD056034 and U54 HD029990 Project 5 (to C.Y.C.).

1. Wong EW, Cheng CY (2009) Polarity proteins and cell-cell interactions in the testis. *Int Rev Cell Mol Biol* 278:309–353.
2. Cheng CY, Mruk DD (2009) An intracellular trafficking pathway in the seminiferous epithelium regulating spermatogenesis: A biochemical and molecular perspective. *Crit Rev Biochem Mol Biol* 44:245–263.
3. Russell L (1977) Movement of spermatocytes from the basal to the adluminal compartment of the rat testis. *Am J Anat* 148:313–328.
4. Yan HH, Mruk DD, Lee WM, Cheng CY (2008) Blood-testis barrier dynamics are regulated by testosterone and cytokines via their differential effects on the kinetics of protein endocytosis and recycling in Sertoli cells. *FASEB J* 22:1945–1959.
5. Wang RS, et al. (2006) Androgen receptor in sertoli cell is essential for germ cell nursery and junctional complex formation in mouse testes. *Endocrinology* 147:5624–5633.
6. Chung NP, Cheng CY (2001) Is cadmium chloride-induced inter-Sertoli tight junction permeability barrier disruption a suitable in vitro model to study the events of junction disassembly during spermatogenesis in the rat testis? *Endocrinology* 142:1878–1888.
7. Meng J, Holdcraft RW, Shima JE, Griswold MD, Braun RE (2005) Androgens regulate the permeability of the blood-testis barrier. *Proc Natl Acad Sci USA* 102:16696–16700.
8. Xia W, Wong EW, Mruk DD, Cheng CY (2009) TGF-β3 and TNFalpha perturb blood-testis barrier (BTB) dynamics by accelerating the clathrin-mediated endocytosis of integral membrane proteins: a new concept of BTB regulation during spermatogenesis. *Dev Biol* 327:48–61.
9. Wong EW, Mruk DD, Lee WM, Cheng CY (2008) Par3/Par6 polarity complex coordinates apical ectoplasmic specialization and blood-testis barrier restructuring during spermatogenesis. *Proc Natl Acad Sci USA* 105:9657–9662.
10. Lui WY, Wong CH, Mruk DD, Cheng CY (2003) TGF-beta3 regulates the blood-testis barrier dynamics via the p38 mitogen activated protein (MAP) kinase pathway: an in vivo study. *Endocrinology* 144:1139–1142.
11. Heasman SJ, Ridley AJ (2008) Mammalian Rho GTPases: New insights into their functions from in vivo studies. *Nat Rev Mol Cell Biol* 9:690–701.
12. Siu MK, Wong CH, Lee WM, Cheng CY (2005) Sertoli-germ cell anchoring junction dynamics in the testis are regulated by an interplay of lipid and protein kinases. *J Biol Chem* 280:25029–25047.
13. Xia W, Mruk DD, Lee WM, Cheng CY (2006) Differential interactions between transforming growth factor-beta3/TbetaR1, TAB1, and CD2AP disrupt blood-testis barrier and Sertoli-germ cell adhesion. *J Biol Chem* 281:16799–16813.
14. Le TL, Yap AS, Stow JL (1999) Recycling of E-cadherin: A potential mechanism for regulating cadherin dynamics. *J Cell Biol* 146:219–232.
15. Morimoto S, et al. (2005) Rab13 mediates the continuous endocytic recycling of occludin to the cell surface. *J Biol Chem* 280:2220–2228.
16. Caswell PT, Vadrevu S, Norman JC (2009) Integrins: masters and slaves of endocytic transport. *Nat Rev Mol Cell Biol* 10:843–853.
17. Siu MK, Mruk DD, Lee WM, Cheng CY (2003) Adhering junction dynamics in the testis are regulated by an interplay of beta 1-integrin and focal adhesion complex-associated proteins. *Endocrinology* 144:2141–2163.
18. Balklava Z, Pant S, Fares H, Grant BD (2007) Genome-wide analysis identifies a general requirement for polarity proteins in endocytic traffic. *Nat Cell Biol* 9:1066–1073.
19. Kroschewski R, Hall A, Mellman I (1999) Cdc42 controls secretory and endocytic transport to the basolateral plasma membrane of MDCK cells. *Nat Cell Biol* 1:8–13.
20. Rojas R, Ruiz WG, Leung SM, Jou TS, Apodaca G (2001) Cdc42-dependent modulation of tight junctions and membrane protein traffic in polarized Madin-Darby canine kidney cells. *Mol Biol Cell* 12:2257–2274.
21. Wu H, Rossi G, Brennwald P (2008) The ghost in the machine: Small GTPases as spatial regulators of exocytosis. *Trends Cell Biol* 18:397–404.
22. Morimoto S, et al. (2005) Rab13 mediates the continuous endocytic recycling of occludin to the cell surface. *J Biol Chem* 280:2220–2228. Q:8
23. Coureuil M, et al. (2009) Meningococcal type IV pili recruit the polarity complex to cross the brain endothelium. *Science* 325:83–87.
24. Cohen D, Müsch A, Rodriguez-Boulan E (2001) Selective control of basolateral membrane protein polarity by cdc42. *Traffic* 2:556–564.
25. Wong EWP, Sun S, Li MWM, Lee WM, Cheng CY (2009) 14-3-3 Protein regulates cell adhesion in the seminiferous epithelium of rat testes. *Endocrinology* 150: 4713–4723.

AUTHOR QUERIES

AUTHOR PLEASE ANSWER ALL QUERIES

Q: 1_Please contact PNAS_Specialist@dartmouthjournals.com if you have questions about the editorial changes, this list of queries, or the figures in your article. Please include your manuscript number in the subject line of all e-mail correspondence; your manuscript number is 201001077. Please (i) review the author affiliation and footnote symbols carefully, (ii) check the order of the author names, and (iii) check the spelling of all author names and affiliations. Please indicate that the author and affiliation lines are correct by adding the comment "OK" next to the author line. Please note that this is your opportunity to correct errors in your article prior to publication. Corrections requested after online publication will be considered and processed as errata.

Q: 2_Please check the order of your key terms and approve or reorder them as necessary.

Q: 3_Please review the information in the author contribution footnote carefully. Please make sure that the information is correct and that the correct author initials are listed. Note that the order of author initials matches the order of the author line per journal style. You may add contributions to the list in the footnote; however, funding should not be an author's only contribution to the work.

Q: 4_You will receive a notification from the PNAS eBill system in 1-2 days. Each corresponding author is required to log in to the system and provide payment information for applicable publication charges (purchase order number or credit card information) upon receipt of the notification. You will have the opportunity to order reprints through the eBill system if desired, as well. Failure to log in and provide the required information may result in publication delays.

Q: 5_Reminder: You have chosen not to pay an additional $1275 (or $950 if your institution has a site license) for the PNAS Open Access option.

Q: 6_Please verify that all supporting information (SI) citations are correct. Note, however, that the hyperlinks for SI citations will not work until the article is published online. In addition, SI that is not composed in the main SI PDF (appendices, datasets, movies, and "Other Supporting Information Files") have not been changed from your originally submitted file and so are not included in this set of proofs. The proofs for any composed portion of your SI are included in this proof as subsequent pages following the last page of the main text. If you did not receive the proofs for your SI, please contact **PNAS_Specialist@dartmouthjournals.com**.

Q: 7_PNAS does not allow statements of novelty or priority. Please rewrite/approve edit.

Q: 8_Duplicate reference is found. Please check reference 22 "Morimoto, et al., 2005", comparing with reference 15.

Supporting Information

Wong et al. 10.1073/pnas.1001077107

SI Materials and Methods

Primary Sertoli Cell Cultures, DNA Transfection, and Cell Staining. Primary Sertoli cells were isolated from 20-d-old rat testes as described (1, 2). Cells were plated at a density of 0.5×10^6 cells/cm^2 on Matrigel-coated dishes (Matrigel:F12/DMEM at 1:7, vol/vol). Two days after isolation, cells were transfected with pCIneo vector control, full-length Cdc42, or dominant-negative mutant T17N plasmid using Effectene transfection reagent (Qiagen). The ratio of DNA to enhancer was 1:8 μL whereas the ratio of DNA to Effectene was at 1 μg:15 μL. A total of 1 μg (12-well plate for cell lysates), 2 μg (6-well plate for endocytosis assay), or 10 μg (100-mm plate for recycling assay) of DNA was transfected. Two days after transfection, cells were treated with or without TGF-β3 (4 ng/mL; Calbiochem) for specified time points and harvested in IP lysis buffer (50 mM Tris, 150 mM NaCl, 1% Nonidet P-40, 2 mM EGTA, 2 mM ethylmaleimide, 10% glycerol, pH 7.4), freshly supplemented with 1 μg/mL aprotinin, 1 μg/mL leupeptin, 2 mM PMSF, and 15 μL/mL each of phosphatase inhibitor mixtures 1 and 2 (Sigma) or cells were subjected to endocytosis or recycling assay. For cell staining, cells were plated at a density of 0.05×10^6 cells/cm^2 on Matrigel-coated coverslips placed in 12-well plate. Transfection was performed as described earlier except that a total of 0.08 μg of fluorescently labeled DNA (Cy3 LabelIT tracker intracellular nucleic acid localization kit; Mirus) was used. Cells were treated with or without TGF-β3 (4 ng/mL) for 1 h before used for immunofluorescence staining.

Preparation of Cdc42 and T17N Mutant cDNA Constructs. Rat full-length Cdc42 (NM_171994) was amplified using the sense primer 5′-CACTCGAGATGCAGACAATTAAGTGTGTTGTTGTTG-3′ and antisense primer 5′-CAGCGGCCGCTCATAGCAGCACACACCTGC-3′ from testis total cDNAs. AccuPrime Taq DNA polymerase (Invitrogen) was used for the PCR. The PCR product was subsequently cloned into the XhoI and NotI sites in the pCIneo vector (Promega). To generate dominant-negative mutant of Cdc42 (T17N), site-directed mutation was performed using the QuikChange XL site-directed mutagenesis kit (Stratagene) according to the manufacturer's protocols. The full-length Cdc42 in pCIneo was used as the template, with the mutagenic primers 5′-GGTGATGGTGCTGTTGGTAAAAACTGTCTCCTGATATCC-3′ (sense) and 5′-GGATATCAGGAGACAGTTTTTACCAACAGCACCATCACC-3′ (antisense). The underlined sequences indicated the mutations introduced, which altered amino acid residue 17 from the N terminus of Cdc42 from Thr (T) to Asn (N). The authenticity of the plasmids was confirmed by direct DNA sequencing at Genewiz. All plasmids were prepared using the HiSpeed Plasmid Midi kit (Qiagen).

Cdc42 Activation Assay. To quantify activated Cdc42 (Cdc42-GTP), primary Sertoli cells were plated at a density of 0.5×10^6 cells/cm^2 on a Matrigel-coated 60-mm dish. Four days thereafter, Sertoli cells were stimulated with or without TGF-β3 (4 ng/mL) for specified time points. Cell lysates were harvested in magnesium lysis/wash buffer (Upstate) freshly supplemented with 10% glycerol, 10 μg/mL aprotinin, and 10 μg/mL leupepetin (MLB buffer). Active Cdc42 was pulled down by recombinant protein corresponding to the p21-binding domain of PAK-1 conjugated to agarose beads (Upstate). Precipitated complex was washed three times by MLB buffer and active Cdc42 was visualized by immunoblotting using a monoclonal anti-Cdc42 antibody (Upstate).

Immunohistochemistry and Fluorescence Microscopy. Frozen testis cross-sections fixed in Bouin fixative were used for immunohistochemistry (3) with the antibody dilutions listed in Table S1. Biotin-conjugated anti–chicken IgY secondary antibody (Abcam) was used before detecting signal with Histostain-SP kit (Zymed Laboratories). Normal chicken IgY (Santa Cruz Biotechnology) served as control. For immunofluorescence microscopy, testis sections were fixed in 4% paraformaldehyde, followed by permeabilization with 0.2% Triton X-100. Sections were mounted in Prolong Gold antifade reagent with DAPI (Invitrogen). All images were acquired with an Olympus BX40 fluorescence microscope and an Olympus DP70 12.5MPa digital camera using the QCapture software (Quantitative Imaging), with the TIFF images imported to PhotoShop (version 10.0.1; Adobe Systems) for overlays and analysis.

Assessment of TJ Permeability Barrier. Sertoli cells were plated on Matrigel-coated bicameral units (Millipore) at 1.2×10^6 cells/cm^2 in triplicate, and the TJ barrier was monitored by TER across the cell epithelium using a Millicell electrical resistance system (Millipore). TGF-β3 (4 ng/mL) was added to both the apical and basal compartments. For overexpression experiments, 0.5 μg DNA was transfected into Sertoli cells in the apical compartment.

Statistical Analysis. Data from treatment groups were compared with the corresponding controls by one-way ANOVA followed by Dunnett test using the GBSTAT Statistical Analysis software package (Dynamic Microsystems). For protein endocytosis experiments, two-way ANOVA followed by Newman-Keuls test was performed. All in vitro experiments were repeated at least three to four times using different batches of Sertoli cells.

SI Discussion

How Does the BTB Maintain Its Integrity During the Transit of Primary Spermatocytes? The BTB is one of the tightest blood–tissue barriers (4). Unlike all other blood–tissue barriers (e.g., the blood–brain barrier), which are constituted by TJ between endothelial cells of the blood capillaries, the BTB is contributed by coexisting TJ, basal ES, and desmosome-gap junction between adjacent Sertoli cells near the basement membrane (5, 6). However, it remains unknown how the BTB attains its plasticity to allow preleptotene spermatocytes in clones and connected by cytoplasmic bridges to traverse the barrier at stage VIII of the epithelial cycle while maintaining immunological barrier integrity (7). Based on recent findings, a hypothetical model has been emerged (4) in which "new" TJ fibrils form behind the spermatocytes in transit to create a "new" BTB before "old" TJ fibrils above the spermatocytes are dissolved. This is mediated by testosterone and/or estrogens which promote the assembly of "new" TJ fibrils by de novo synthesis of junction proteins (8–11) and/or transcytosis (12) of proteins from intercellular junction sites above the transiting spermatocytes. "Old" TJ-fibrils above the spermatocytes will then be "dissolved" under the influence of cytokines (e.g., TGF-β3), which increase the clathrin-mediated endocytosis of the integral membrane proteins (12, 13). Internalized proteins will be targeted to the "new" BTB site by testosterone or undergone endosome-mediated degradation (12). This thus allows the transit of spermatocytes at the BTB while maintaining the immunological barrier. However, the mechanism (s) that control these complex protein trafficking events are just beginning to be unveiled. Here, we have demonstrated that the TGF-β3–induced disruption of the "old" BTB above the spermatocytes in transit is facilitated by an increase in protein endo-

cytosis, but this process is tightly regulated by Cdc42. As Cdc42 is also detected at the apical ES, it is likely that it also plays a role in modulation spermiation as this event and BTB restructuring take place simultaneously at the opposite ends of the epithelium at stage VIII of the epithelial cycle. As such, Cdc42 plausibly serves as the molecular "switch" to coordinate these events.

Transient Activation of Sertoli Cell Cdc42 in Response to TGF-β3 Treatment. The transient activation of Cdc42 in response to TGF-β3 as shown in Fig. 2 in the main text is intriguing. However, it is noted that, in addition to this observation having been seen repeatedly in multiple experiments using different batches of Sertoli cells, this finding is consistent with data in the literature. For instance, Edlund et al. reported that after treatment of prostate cancer cell line PC-3U with TGF-β and cadmium chloride, there was an activation of Cdc42 soon after treatment at 5 to 15 min (14). However, further treatment up to 2 h resulted in an inactivation of Cdc42. Interestingly, a second wave of activation was observed at 6 h posttreatment. In our study as reported herein, we did not investigate if Cdc42 was activated after Sertoli cells were treated with TGF-β for as long as several hours. However, we speculate that activation of Cdc42 is a transient but prerequisite event to facilitate protein endocytosis mediated by TGF-β3. This is consistent with the normal mode of action of small GTPases whereby they are activated transiently to transduce signals to downstream effectors, to be followed by their rapid inactivation to prevent unwanted stimulation of other signaling pathways. Therefore, even though the phenotypic changes (such as redistribution of junction proteins from the cell–cell interface to cell cytosol, and a significant decline in Sertoli cell TJ permeability barrier when quantified by TER across the cell epithelium) were observed after the activation of Cdc42, it is physiologically significant. In addition, overexpression of dominant negative form of Cdc42 reversed the disruptive effects caused by TGF-β3, which provides direct evidence indicating activation of Cdc42 is involved in mediating the damaging effects by TGF-β on the Sertoli cell BTB.

1. Wong EWP, Cheng CY (2009) Polarity proteins and cell-cell interactions in the testis. *Int Rev Cell Mol Biol* 278:309–353.
2. Wong EW, Mruk DD, Lee WM, Cheng CY (2008) Par3/Par6 polarity complex coordinates apical ectoplasmic specialization and blood-testis barrier restructuring during spermatogenesis. *Proc Natl Acad Sci USA* 105:9657–9662.
3. Siu MK, Wong CH, Lee WM, Cheng CY (2005) Sertoli-germ cell anchoring junction dynamics in the testis are regulated by an interplay of lipid and protein kinases. *J Biol Chem* 280:25029–25047.
4. Cheng CY, Mruk DD (2009) An intracellular trafficking pathway in the seminiferous epithelium regulating spermatogenesis: A biochemical and molecular perspective. *Crit Rev Biochem Mol Biol* 44:245–263.
5. Rojas R, Ruiz WG, Leung SM, Jou TS, Apodaca G (2001) Cdc42-dependent modulation of tight junctions and membrane protein traffic in polarized Madin-Darby canine kidney cells. *Mol Biol Cell* 12:2257–2274.
6. Wong EW, Cheng CY (2009) Polarity proteins and cell-cell interactions in the testis. *Int Rev Cell Mol Biol* 278:309–353.
7. Mruk DD, Cheng CY (2008) Delivering non-hormonal contraceptives to men: Advances and obstacles. *Trends Biotechnol* 26:90–99.
8. Wang RS, et al. (2006) Androgen receptor in Sertoli cell is essential for germ cell nursery and junctional complex formation in mouse testes. *Endocrinology* 147: 5624–5633.
9. Chung NP, Cheng CY (2001) Is cadmium chloride-induced inter-Sertoli tight junction permeability barrier disruption a suitable in vitro model to study the events of junction disassembly during spermatogenesis in the rat testis? *Endocrinology* 142:1878–1888.
10. Meng J, Holdcraft RW, Shima JE, Griswold MD, Braun RE (2005) Androgens regulate the permeability of the blood-testis barrier. *Proc Natl Acad Sci USA* 102:16696–16700.
11. MacCalman CD, Getsios S, Farookhi R, Blaschuk OW (1997) Estrogens potentiate the stimulatory effects of follicle-stimulating hormone on N-cadherin messenger ribonucleic acid levels in cultured mouse Sertoli cells. *Endocrinology* 138:41–48.
12. Yan HH, Mruk DD, Lee WM, Cheng CY (2008) Blood-testis barrier dynamics are regulated by testosterone and cytokines via their differential effects on the kinetics of protein endocytosis and recycling in Sertoli cells. *FASEB J* 22:1945–1959.
13. Xia W, Wong EW, Mruk DD, Cheng CY (2009) TGF-β3 and TNFalpha perturb blood-testis barrier (BTB) dynamics by accelerating the clathrin-mediated endocytosis of integral membrane proteins: a new concept of BTB regulation during spermatogenesis. *Dev Biol* 327:48–61.
14. Edlund S, et al. (2003) Transforming growth factor-beta1 (TGF-beta)-induced apoptosis of prostate cancer cells involves Smad7-dependent activation of p38 by TGF-beta-activated kinase 1 and mitogen-activated protein kinase kinase 3. *Mol Biol Cell* 14:529–544.
15. Wray W, Boulikas T, Wray VP, Hancock R (1981) Silver staining of proteins in polyacrylamide gels. *Anal Biochem* 118:197–203.

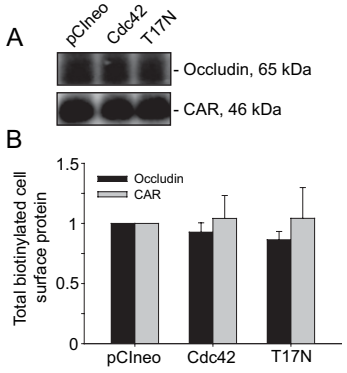

Fig. S1. Analysis of total biotinylated proteins on cell surface of Sertoli cells. (*A*) Proteins at the cell surface of Sertoli cells expressing vector control (pCIneo), Cdc42, or dominant-negative Cdc42 (T17N) were biotinylated. Biotinylated proteins were recovered by NeutrAvidin in the pull-down assay and occludin or CAR was visualized by immunoblotting using corresponding specific antibody. Equal amount of occludin and CAR were observed at the cell surface of control, Cdc42, or T17N expressing cells. (*B*) Composite results from three independent experiments were shown that illustrate an insignificant change in total cell surface biotinylated protein levels of occludin and CAR.

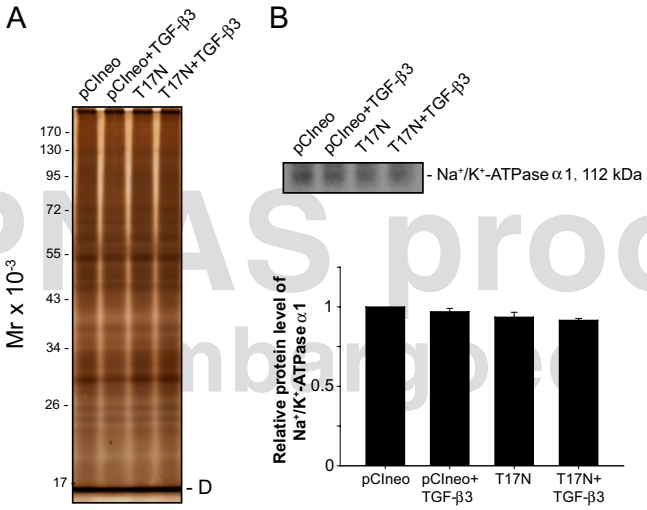

Fig. S2. An analysis to verify that similar amount of protein was used in recycling assay. Silver nitrate–stained gel illustrating equal amount of protein was used in recycling assay. Recycling assay and plasma membrane extraction was performed as described in *Materials and Methods*. To illustrate that equal amount of protein was used in the affinity precipitation step to quantify the levels of selected proteins that were recycled to cell surface, proteins were resolved by SDS/PAGE and the gel was stained with silver nitrate as described (15) (*A*). (*B*) To further confirm that equal amount of plasma membrane proteins was used for affinity precipitation, immunoblotting was performed using a plasma membrane marker sodium/potassium ATPase α1 (Na^+/K^+-ATPase α1). Lower panel is a composite result of two independent experiments by immunoblotting, such as the one shown in the upper panel.

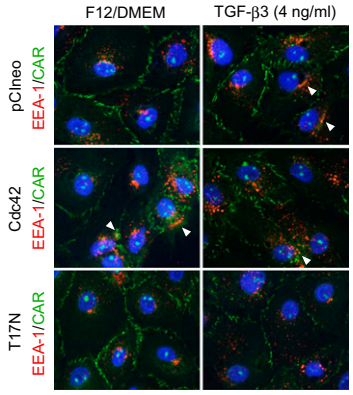

Fig. S3. Dual-labeled immunofluorescence analysis to assess cellular distribution of CAR and an endocytic vesicle marker early endosome antigen–1 (EEA-1). Sertoli cells were transfected with vector control (pCIneo), Cdc42, or T17N on day 2 after isolation after an intact cell epithelium was established with a functional TJ permeability barrier. Two days after transfection, cells were treated with or without 4 ng/mL of TGF-β3 for 60 min. Thereafter, cells were fixed with 4% paraformaldehyde and stained with an anti-CAR antibody (green) and an anti–EEA-1 antibody (red). Nuclei were visualized by DAPI (blue). Consistent with Fig. 6 *B* and *C* in the main text, overexpression of Cdc42 caused a redistribution of CAR from the cell–cell interface to cytosol compared with vector control pCIneo. Interestingly, the redistributed CAR protein colocalized with EEA-1 (white arrowheads), indicating that the internalized CAR protein was sorted into the early endosome. In addition, similar to the previous results (13), treatment of Sertoli cells with TGF-β3 disrupted the localization of CAR at the cell–cell interface. Concomitantly, internalized CAR protein colocalized with EEA-1. This change was observed in both control and Cdc42 overexpressed cells, but not Sertoli cells that expressed T17N.

Table S1. Antibodies used for different experiments in this report

Antibody (host animal)	Vendor	Catalog no.	Application/working dilution	Fixation
Goat anti-actin	Santa Cruz Biotechnology	sc-1616	WB (1:200)	—
Mouse anti-occludin	Zymed Laboratories	33–1,500	IF (1:50)	—
Mouse anti-γ-catenin	BD Transduction Laboratories	610254	WB (1:1,000) IF (1:75)	—
Rabbit anti-occludin	Zymed Laboratories	71–1500	WB (1:150)	—
Rabbit anti-ZO-1	Zymed Laboratories	61–7300	WB (1:150)	4% PFA (IF)
Rabbit anti-N-cadherin	Santa Cruz Biotechnology	sc-7939	WB (1:200) IF (1:50)	4% PFA (IF)
Rabbit anti-α-catenin	Santa Cruz Biotechnology	sc-7894	WB (1:200) IF (1:50)	—
Rabbit anti-β-catenin	Santa Cruz Biotechnology	sc-7199	WB (1:200) IF (1:50)	—
Rabbit anti-γ-catenin	Santa Cruz Biotechnology	sc-7900	WB (1:200)	—
Chicken anti-Cdc42	Abcam	ab17437	WB (1:3,000) IHC (1:100) IF (1:75)	Bouin fixative (IHC) 4% PFA (IF)
Mouse anti-Cdc42	Upstate Biotechnology	05–542	WB (1:250)	—
Rabbit anti-CAR	Santa Cruz Biotechnology	sc-15405	WB (1:200) IF (1:50)	Methanol (IF) 4% PFA (IF)
Mouse anti-EEA-1	BD Transduction Laboratories	610456	IF (1:50)	4% PFA (IF)
Mouse anti-Na^+/K^+ -ATPase α1	Abcam	ab7671	WB (1:2,500)	—

IF, immunofluorescent microscopy; IHC, immunohistochemistry; IP, immunoprecipitation; PFA, paraformaldehyde; WB, Western blotting.

AUTHOR QUERIES

AUTHOR PLEASE ANSWER ALL QUERIES

There are no queries in this article.